Non-redundant roles of cathepsins in promoting necrosis of human macrophages

Małgorzata Kalinka[1], Julia Nguyen[1], Maria Łęcka[1], Vanessa Pippa[1], Boris Turk[3,4], Guy S. Salvesen[2], Katarzyna Groborz[1,2,*], Marcin Poręba[1,5,*]

[1]Faculty of Chemistry, Wroclaw University of Science and Technology, 50-370 Wroclaw, Poland; [2]SBP Medical Discovery Institute, La Jolla, 92037, CA, USA; [3]Jozef Stefan Institute, Ljubljana, 1000, Slovenia; [4]Faculty of Chemistry and Chemical Engineering, University of Ljubljana, 1000 Ljubljana, Slovenia; [5]Faculty of Medicine, Wroclaw University of Science and Technology, 50-370 Wroclaw, Poland; *correspondence: katarzyna.groborz@gmail.com, marcin.poreba@pwr.edu.pl

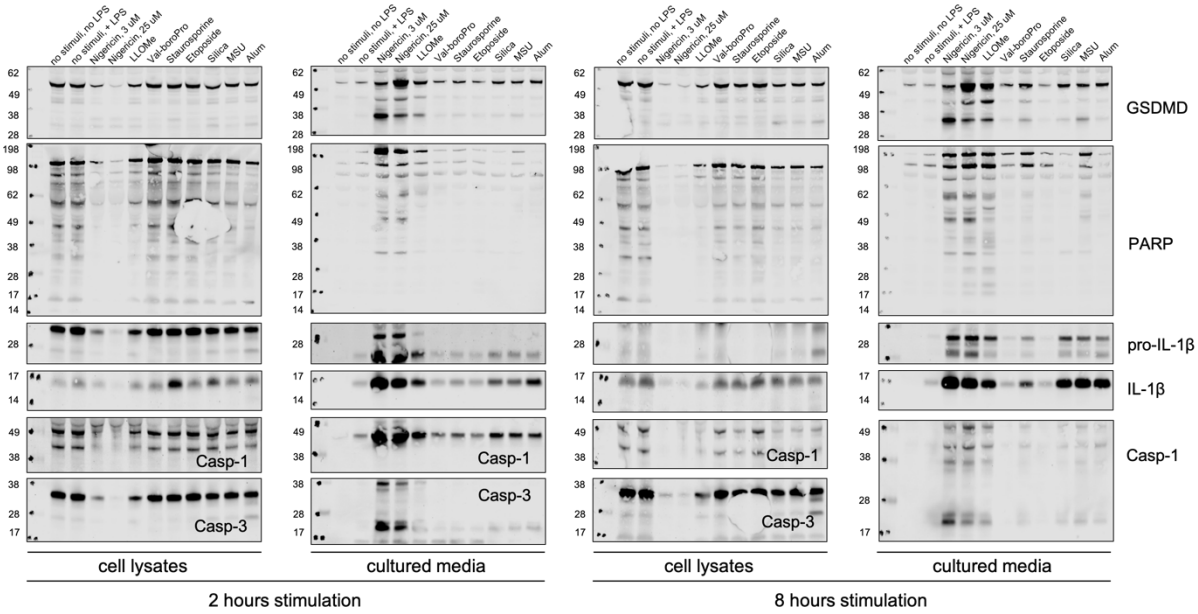

Supplementary Fig. 1 In relation to Figure 1. Cleavage patterns of GSDMD, PARP, IL-1β, caspase-1, and caspase-3 in LPS-primed THP-1 cells treated with the indicated stimuli: nigericin (3 μM or 25 μM), L-leucyl-L-leucine methyl ester (LLOMe), Val-boroPro, staurosporine, etoposide, silica (SiO_2), monosodium urate (MSU), or alum [$Al(OH)_3$]. Immunoblots of cell lysates and culture supernatants show proteolytic fragments after 2 h and 8 h of stimulation.

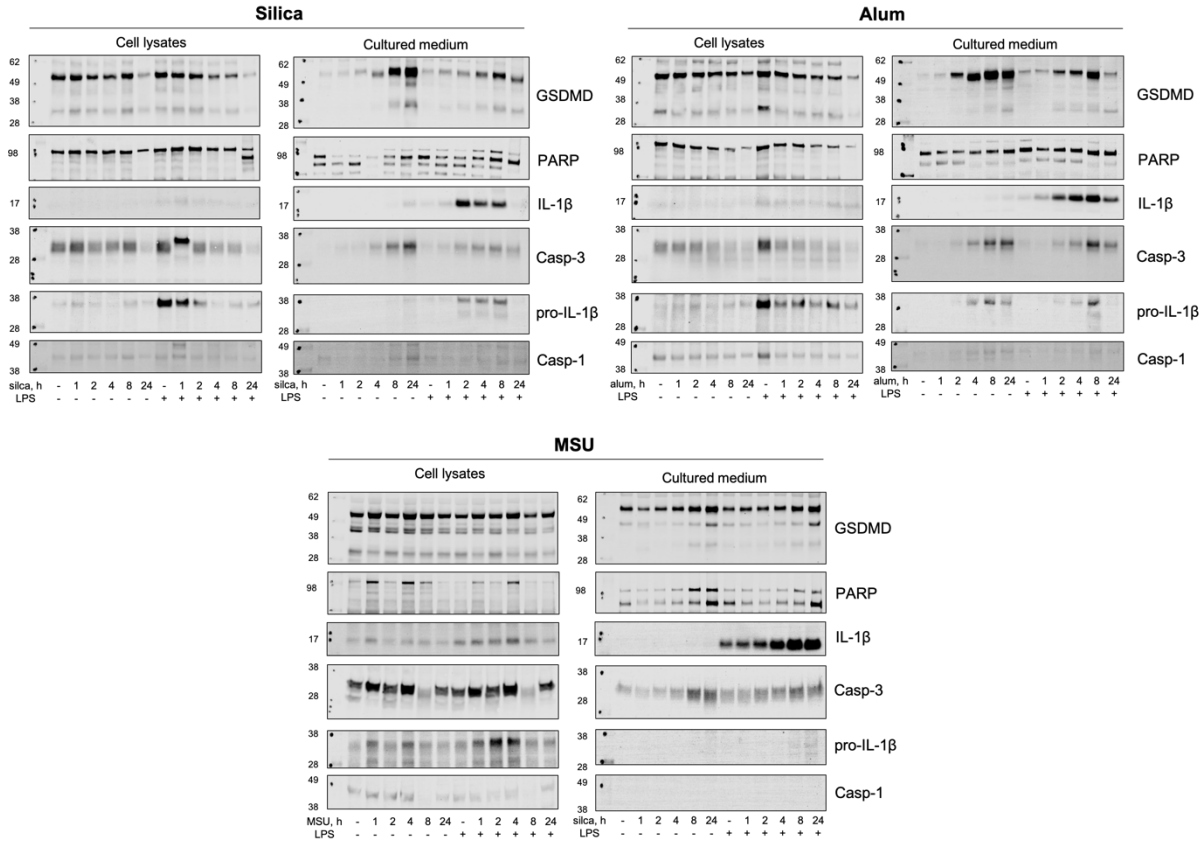

Supplementary Fig. 2 In relation to Figure 1. Cleavage patterns of GSDMD, PARP, (pro)IL-1β, caspase-1, and caspase-3 in THP-1 cells ± LPS priming, treated with silica (SiO_2), alum [$Al(OH)_3$], or monosodium urate (MSU) to model sterile inflammation. Immunoblots of cell lysates and culture supernatants show proteolytic fragments over a time course up to 24 h.

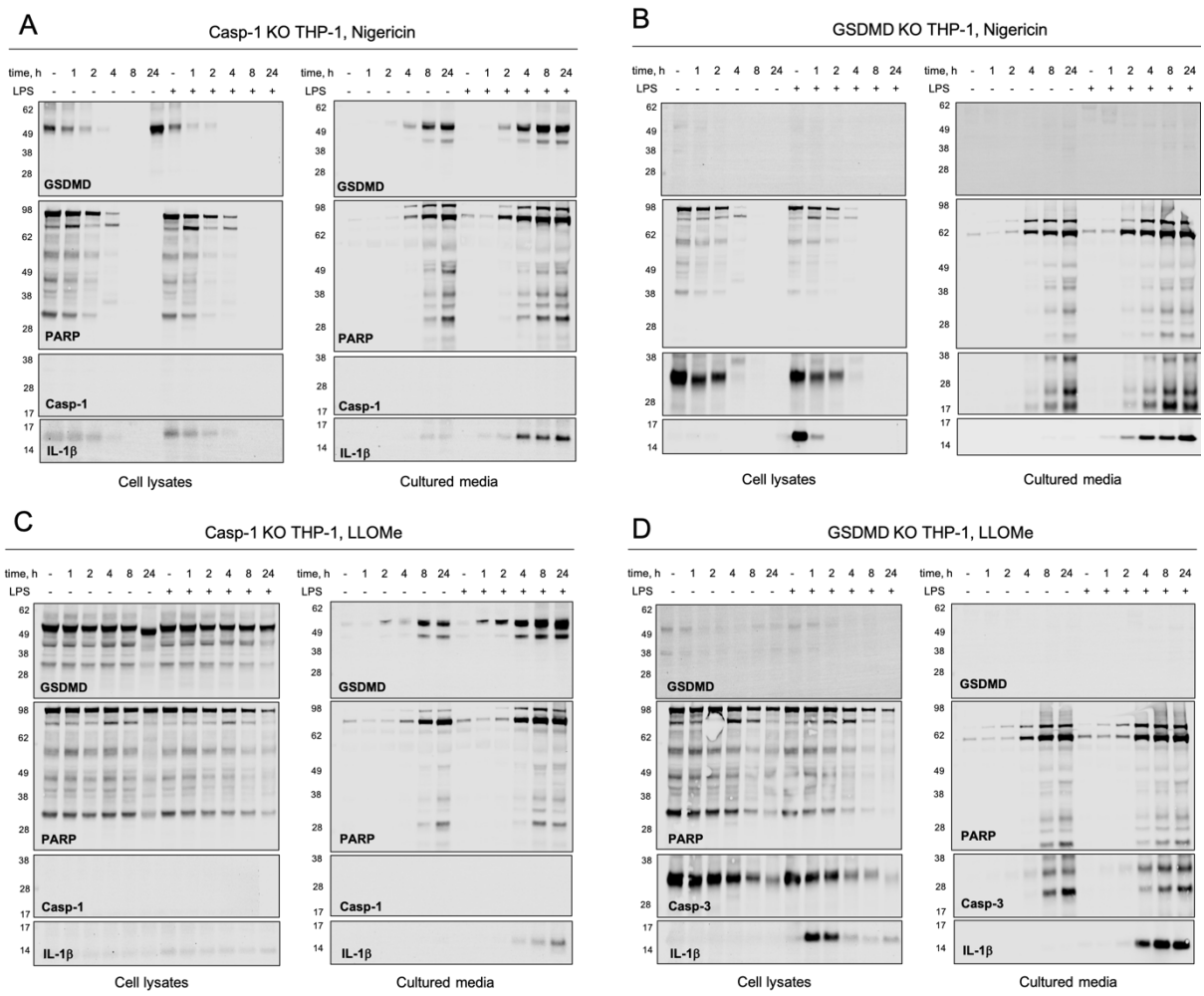

Supplementary Fig. 3 In relation to Figure 2 Cell death signatures in PMA-differentiated caspase-1- and GSDMD-deficient THP-1 cells. Western blot analysis showing the processing patterns of GSDMD, PARP, and pro-IL-1β in response to nigericin (A, B) and LLOMe (C, D) stimulation in caspase-1 KO (A, C) and GSDMD KO (B, D) THP-1 cells. Key features include GSDMD cleavage by caspase-1 (p31 fragment) or by caspase-3 (p45 fragment), and PARP processing via either the canonical apoptotic pathway (caspase-3; p89 and p25 fragments) or non-canonical cleavage by cysteine cathepsins (p55 and p42 fragments). Notably, pro-IL-1β was processed and secreted as its mature form even in the absence of caspase-1, highlighting the contribution of alternative proteolytic pathways to cytokine activation.

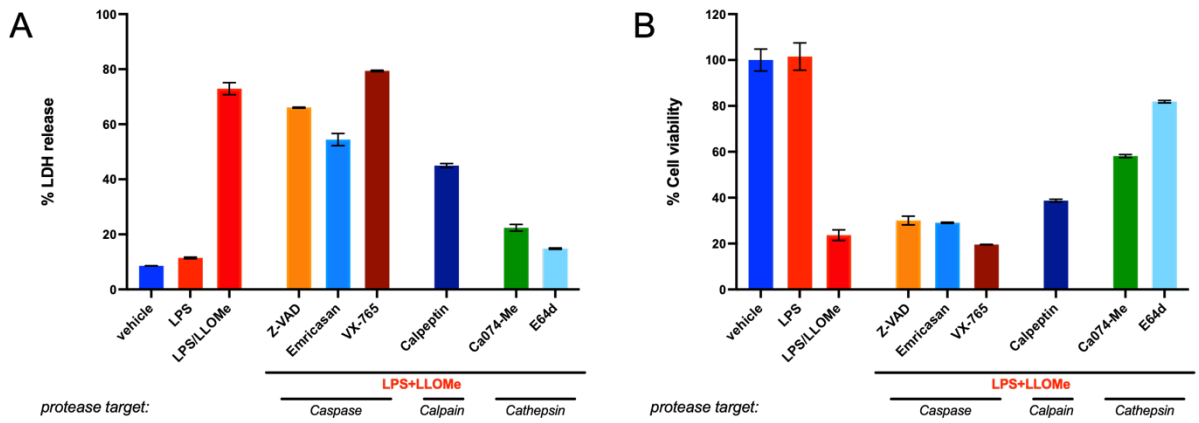

Supplementary Fig. 4 In relation to Figure 3 LLOMe induces lytic cell death in PMA-primed, LPS-stimulated THP-1 cells. (A) shows LDH release (%), and (B) shows cell viability (%), following stimulation with LPS/LLOMe in the presence or absence of the indicated inhibitors: zVAF-fmk, emricasan, or VX-765 (caspases); calpeptin (calpain-1); and CA074Me or E64d (lysosomal cathepsins).

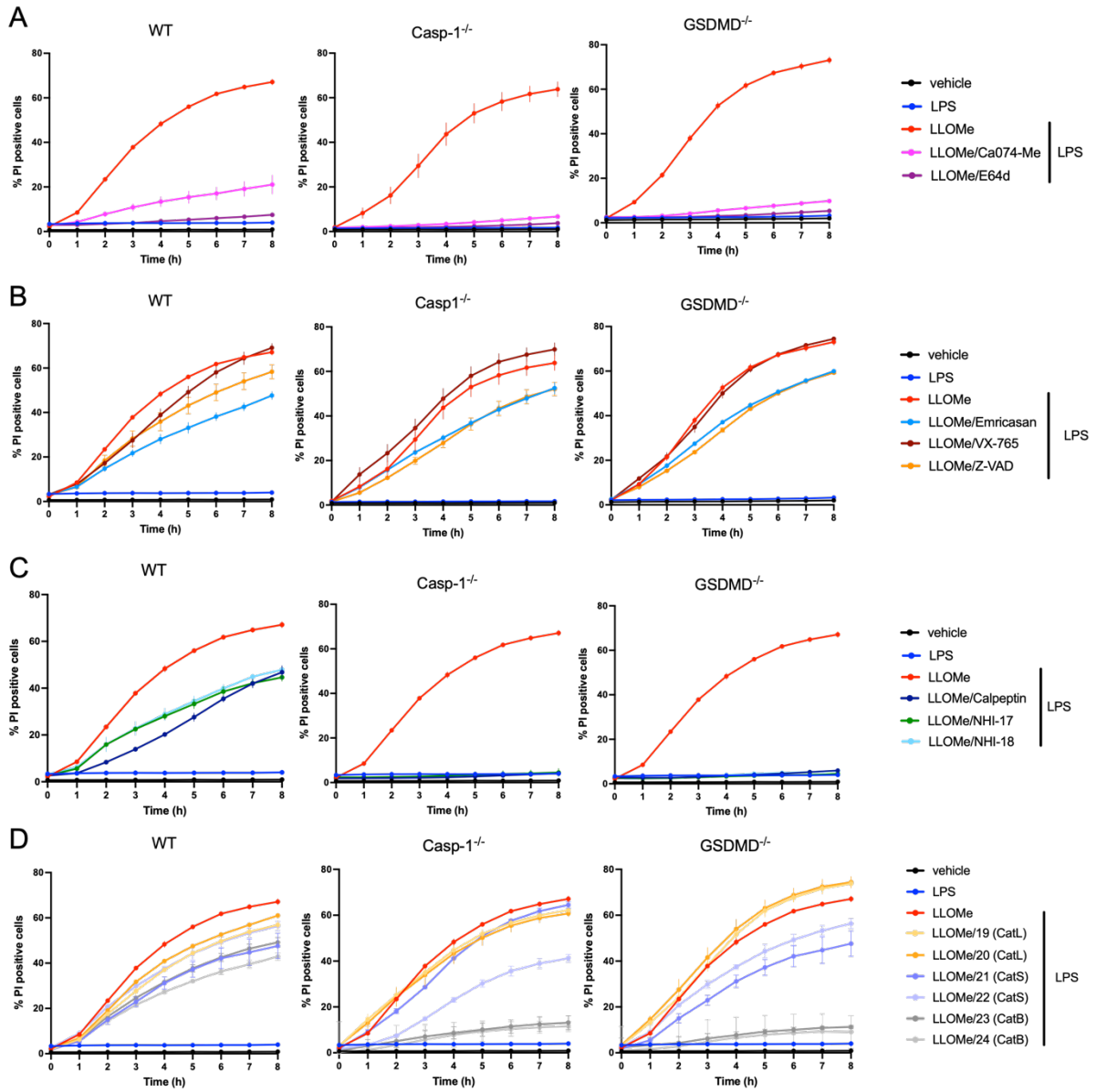

Supplementary Fig. 5 In relations to Figure 3 Time-course analysis of PI uptake in LPS-primed M0 THP-1 cells treated with LLOMe (500 μM) in the presence of; (A) pan-cathepsin inhibitors CA-074Me or E64d; (B) caspase inhibitors emricasan, VX-765, or zVAD-fmk; (C) calpeptin; and (D) cathepsin-selective inhibitors (CatL-19, CatL-20, CatS-21, CatS-22, CatB-23, CatB-24).

Supplementary Table 1 The structure of cathepsin S inhibitors. In relation to Figure 3.

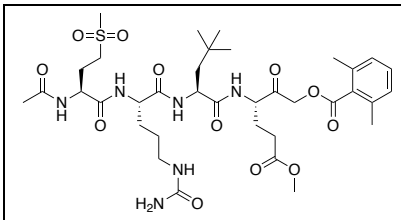 JN-1 Ac-Met(O_2)-Cit-NptGly-Glu(Me)-AOMK	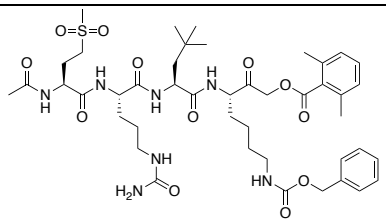 JN-2 Ac-Met(O_2)-Cit-NptGly-Lys(2ClZ)-AOMK	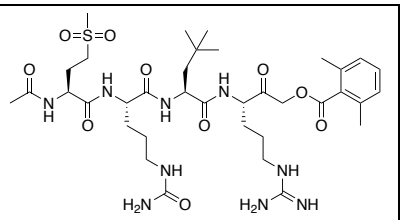 JN-3 Ac-Met(O_2)-Cit-NptGly-Arg-AOMK

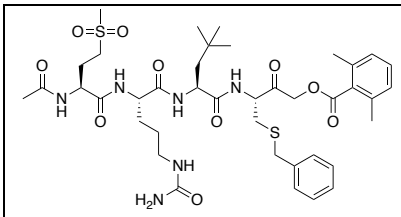 JN-4 Ac-Met(O_2)-Cit-NptGly-Cys(Bzl)-AOMK	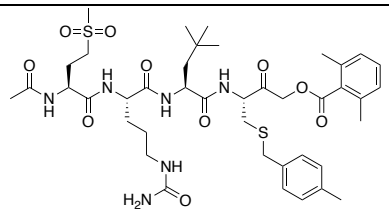 JN-5 Ac-Met(O_2)-Cit-NptGly-Cys(MeBzl)-AOMK	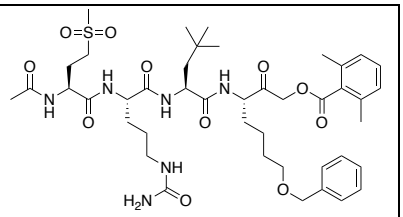 JN-6 Ac-Met(O_2)-Cit-NptGly-Nle(OBzl)-AOMK
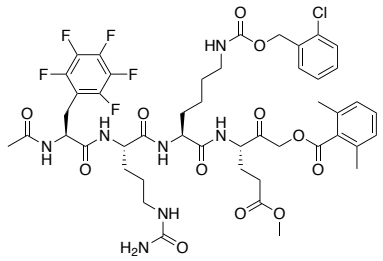 JN-7 Ac-Phe(F_5)-Cit-Lys(2ClZ)-Glu(Me)-AOMK	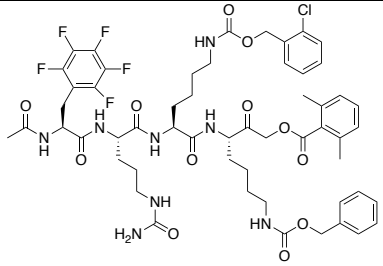 JN-8 Ac-Phe(F_5)-Cit-Lys(2ClZ)-Lys(2ClZ)-AOMK	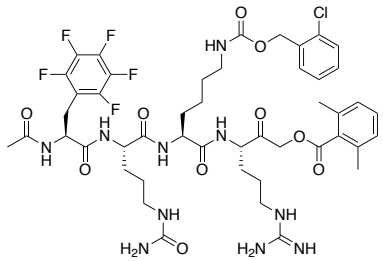 JN-9 Ac-Phe(F_5)-Cit-Lys(2ClZ)-Arg-AOMK
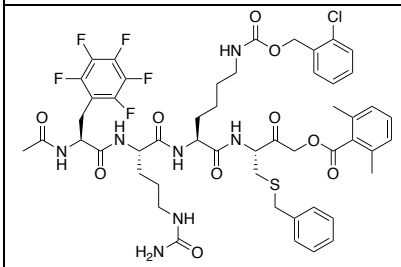 JN-10 Ac-Phe(F_5)-Cit-Lys(2ClZ)-Cys(Bzl)-AOMK	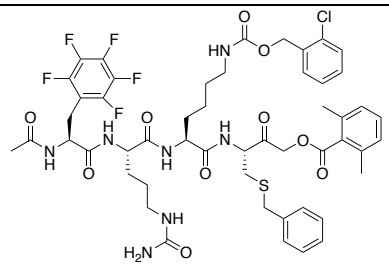 JN-11 Ac-Phe(F_5)-Cit-Lys(2ClZ)-Cys(MeBzl)-AOMK	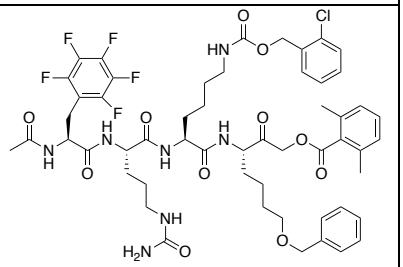 JN-12 Ac-Phe(F_5)-Cit-Lys(2ClZ)-Nle(OBzl)-AOMK

Supplementary Table 2. The structure of cathepsin B and cathepsin L inhibitors. In relation to Figure 3.

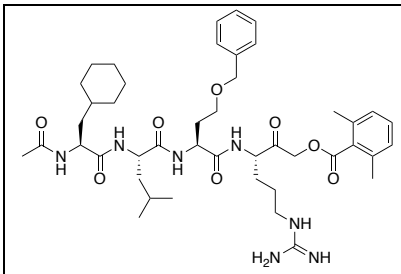 VP-1 Ac-Cha-Leu-hSer(Bzl)-Arg-AOMK	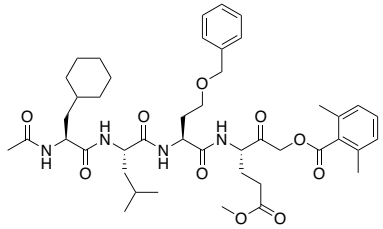 VP-2 Ac-Cha-Leu-hSer(Bzl)-Glu(Me)-AOMK	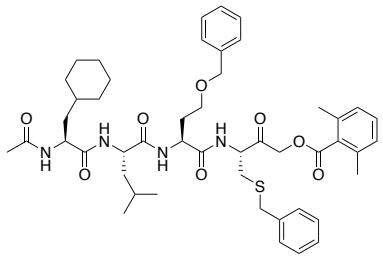 VP-3 Ac-Cha-Leu-hSer(Bzl)-Cys(Bzl)-AOMK
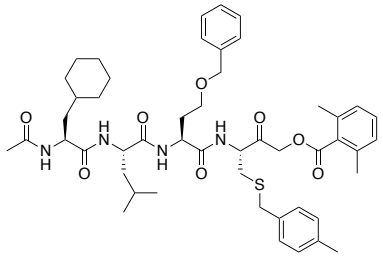 VP-4 Ac-Cha-Leu-hSer(Bzl)-Cys(MeBzl)-AOMK	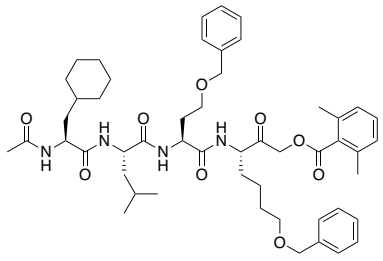 VP-5 Ac-Cha-Leu-hSer(Bzl)-Nle(OBzl)-AOMK	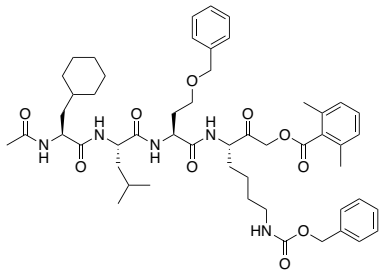 VP-6 Ac-Cha-Leu-hSer(Bzl)-Lys(2ClZ)-AOMK

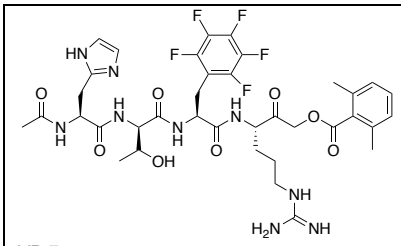

VP-7
Ac-His-DThr-Phe(F_5)-Arg-AOMK

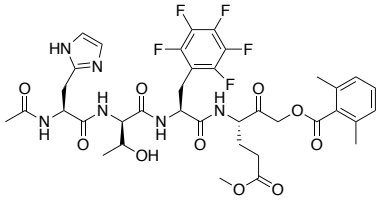

VP-7
Ac-His-DThr-Phe(F_5)-Glu(Me)-AOMK

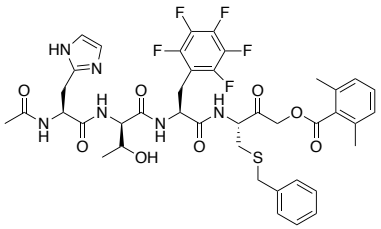

VP_9
Ac-His-DThr-Phe(F_5)-Cys(Bzl)-AOMK

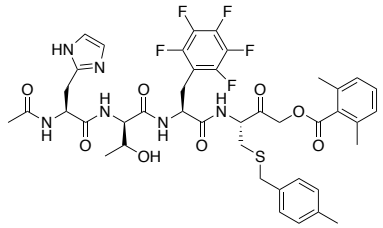

VP-10
Ac-His-DThr-Phe(F_5)-Cys(MeBzl)-AOMK

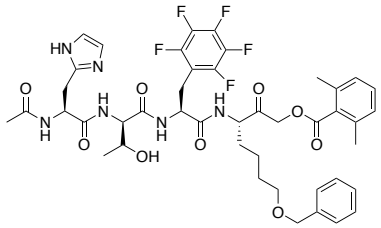

VP-11
Ac-His-DThr-Phe(F_5)-Nle(OBzl)-AOMK

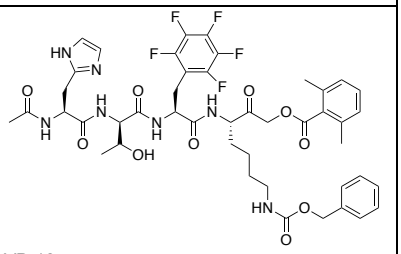

VP-12
Ac-His-DThr-Phe(F_5)-Lys(2ClZ)-AOMK

Supplementary Table 3. Kinetic parameters of cathepsin inhibitors. In relation to Figure 3.

P4-P2	P1	Code	$k_{obs}/[I]$, $M^{-1}s^{-1}$		
			Cathepsin S	Cathepsin L	Cathepsin B
Cha-Leu-hSer(Bzl)	Arg	**VP-1**	3,700	2,700	**1,790,000**
	Glu(Me)	**VP-2**	760	rev. < 1,000	**883,000**
	Cys(Bzl)	**VP-3**	180	rev. < 1,000	**174,000**
	Cys(MeBzl)	**VP-4**	130	rev. < 1,000	**106,000**
	Nle(OBzl)	**VP-5**	460	rev. < 1,000	**173,000**
	Lys(2ClZ)	**VP-6**	570	rev. < 1,000	**2,200**
His-DThr-Phe(F5)	Arg	**VP-7**	20	**69,900**	1,400
	Glu(Me)	**VP-8**	1,100	**26,600**	2,300
	Cys(Bzl)	**VP-9**	710	**45,500**	3,900
	Cys(MeBzl)	**VP-10**	220	**29,600**	480
	Nle(OBzl)	**VP-11**	700	**32,200**	42,00
	Lys(2ClZ)	**VP-12**	900	**17,400**	830
Met(O_2)-Cit-NptGly	Glu(Me)	**JN-1**	**392,000**	560	7,440
	Lys(2ClZ)	**JN-2**	**269,000**	220	5,100
	Arg	**JN-3**	**236,000**	4,840	41,500
	Cys(Bzl)	**JN-4**	**443,000**	450	22,400
	Cys(MeBzl)	**JN-5**	**344,000**	610	10,500
	Nle(OBzl)	**JN-6**	**246,000**	650	16,900
Phe(F_5)-Cit-Lys(2ClZ)	Glu(Me)	**JN-7**	**609,999**	870	17,000
	Lys(2ClZ)	**JN-8**	**225,000**	350	1,600
	Arg	**JN-9**	**371,000**	4,270	148,000
	Cys(Bzl)	**JN-10**	**545,000**	620	16,100
	Cys(MeBzl)	**JN-11**	**261,000**	320	1,900
	Nle(OBzl)	**JN-12**	**392,000**	490	5,160
		E-64	132,000	65,100	81,200

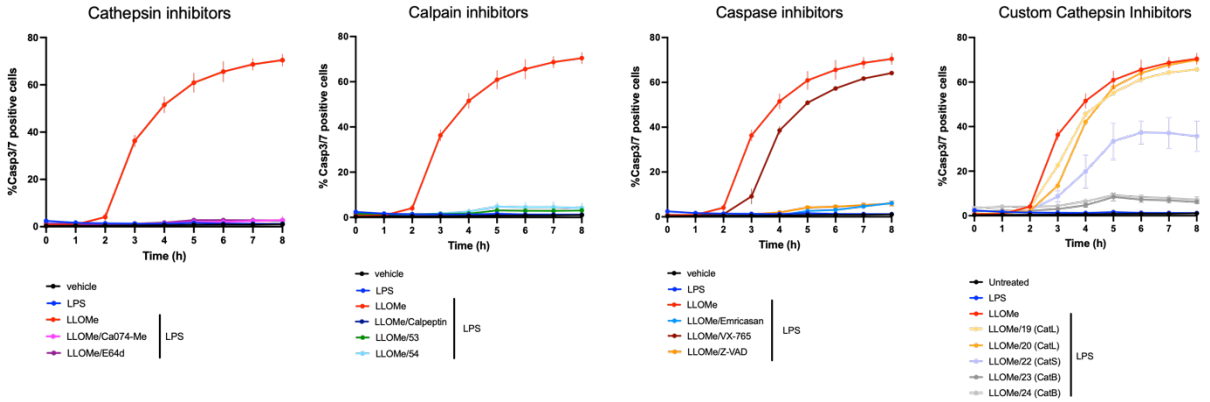

Supplementary Figure 6. In relations to Figure 3 Time-course analysis of DEVD-ase activity in LPS-primed M0 THP-1 cells treated with LLOMe (500 μM) in the presence of pan-cathepsin inhibitors (CA-074Me or E64d); calpain-1 inhibitors (calpeptin, NHI-17, NHI-18); caspase inhibitors (emricasan, VX-765, zVAD-fmk); and cathepsin-selective inhibitors (CatL-19, CatL-20, CatS-21, CatS-22, CatB-23, CatB-24).

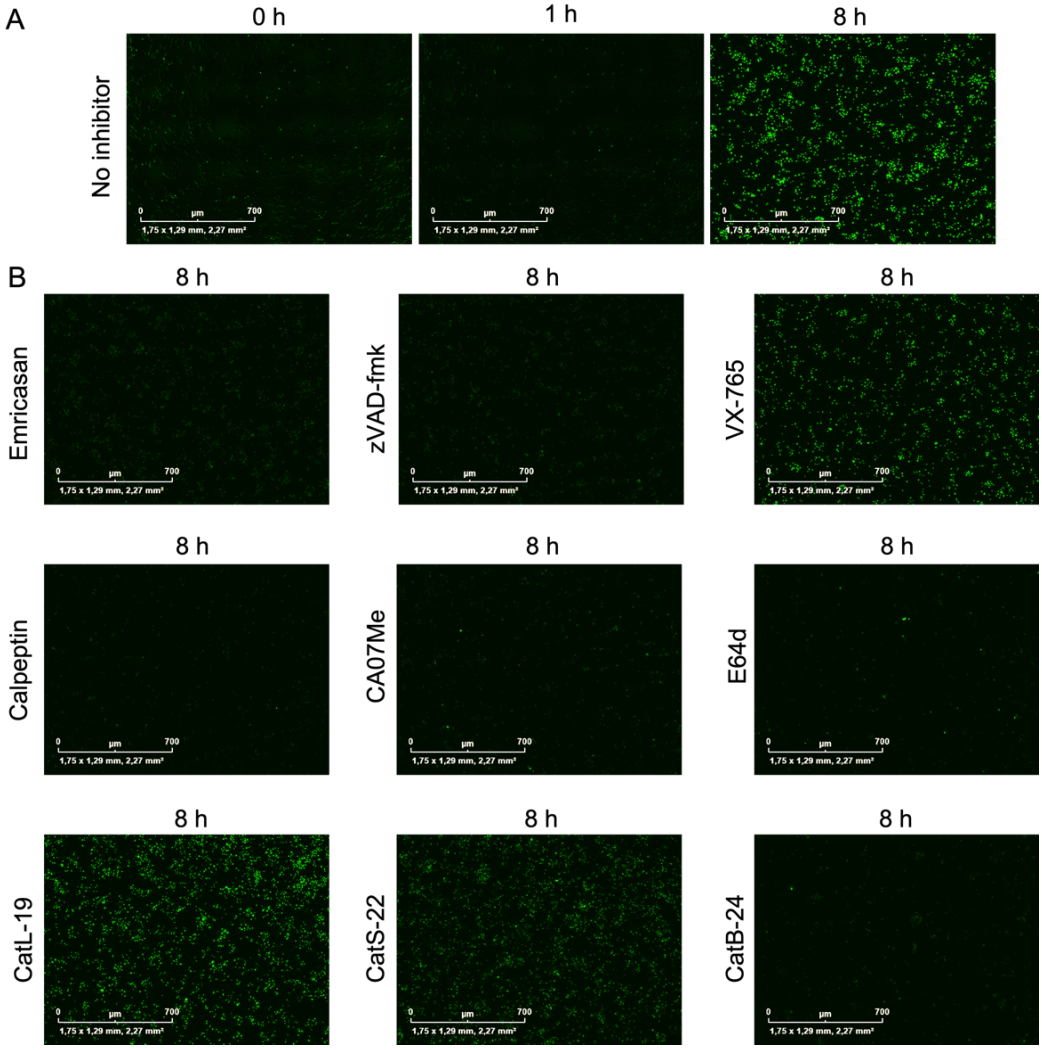

Supplementary Figure 7. Caspase-3/7 activation in LPS/LLOMe-treated WT M0 THP-1 cells. (A) Representative fluorescence images of caspase-3/7 activity in stimulated cells with no inhibitor at 0, 1,

and 8 h. (B) Representative fluorescence images of caspase-3/7 activity after 8 h of stimulation in cells pretreated with the indicated inhibitors (25 μM, 2 h prior stimulation).

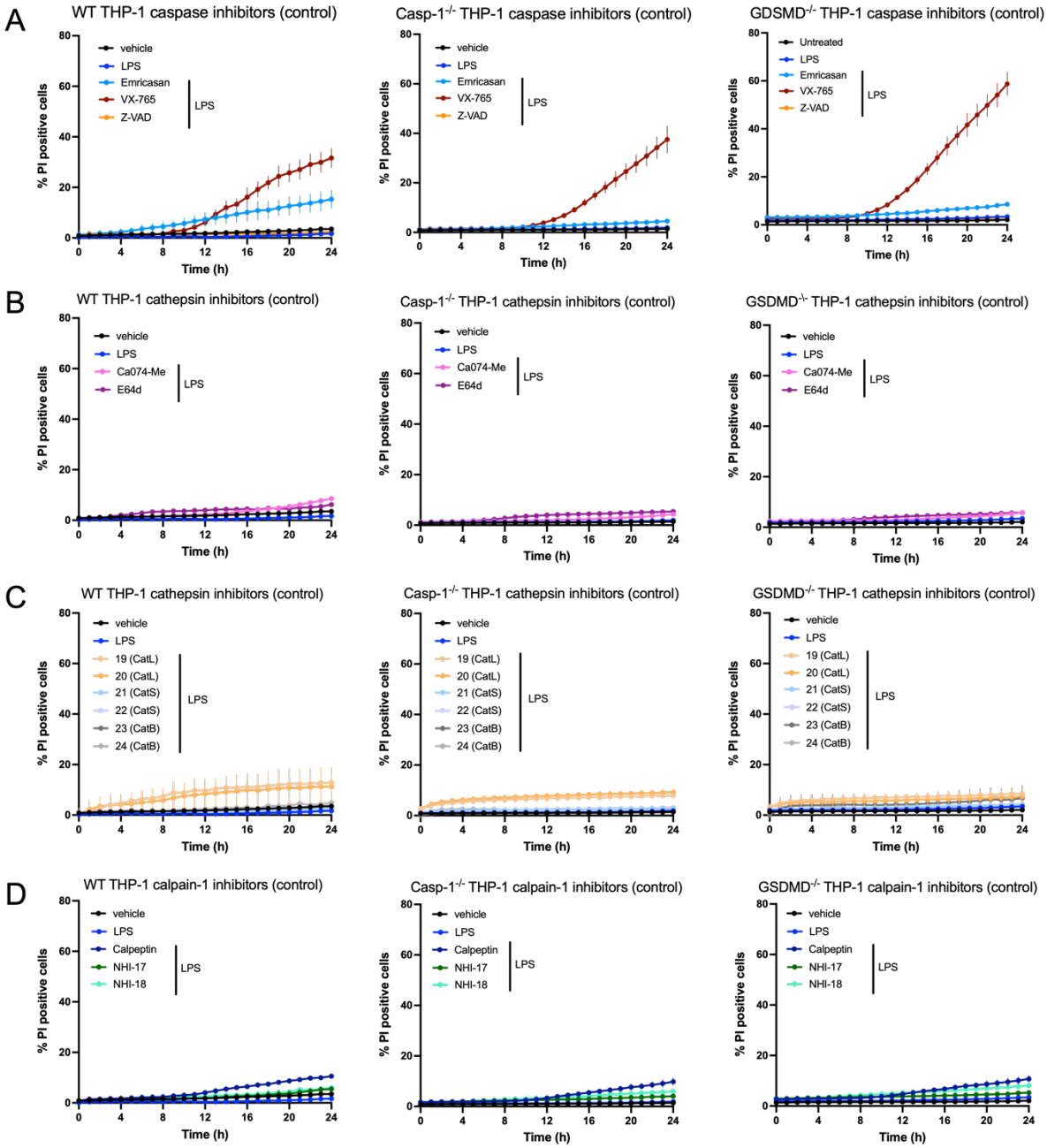

Supplementary Figure 8. In relations to Figure 3. Time-course analysis of PI uptake in LPS-primed M0 THP-1 cells (WT, Casp-1$^{-/-}$, and GSDMD$^{-/-}$) without cell death stimulants in the presence of (A) caspase inhibitors (emricasan, VX-765, zVAD-fmk), (B) pan-cathepsin inhibitors (CA-074Me or E64d), (C) cathepsin-selective inhibitors (CatL-19, CatL-20, CatS-21, CatS-22, CatB-23, CatB-24), and calpain-1 inhibitors (calpeptin, NHI-17, NHI-18).

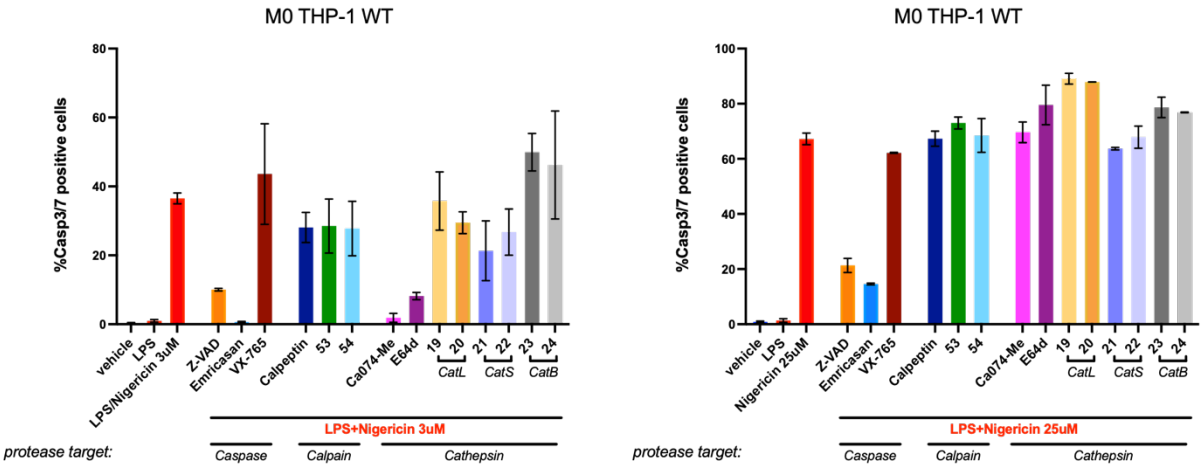

Supplementary Figure 9. In relation to Figure 4. DEVD-ase activity in M0 WT THP-1 cells following 3 μM and 25 μM nigericin in the presence of pan-caspase (zVAD, Emricasan), caspase-1 selective (VX-765), calpain-1 (Calpeptin), or cathepsin inhibitors (CA-074Me, E64d, CatL-19, CatL-20, CatS-21, CathS-22, CatB-23, CathB-24).